Liquid Crystals
Publication details, including instructions for authors and subscription information:
http://www.informaworld.com/smpp/title~content=t713926090

Detailed experimental investigation on recording of switchable diffraction gratings in polymer dispersed liquid crystal films by UV laser curing

D. Duca; A. V. Sukhov; C. Umeton

Online publication date: 06 August 2010

To cite this Article Duca, D. , Sukhov, A. V. and Umeton, C.(1999) 'Detailed experimental investigation on recording of switchable diffraction gratings in polymer dispersed liquid crystal films by UV laser curing', Liquid Crystals, 26: 6, 931 — 937
To link to this Article: DOI: 10.1080/026782999204633
URL: http://dx.doi.org/10.1080/026782999204633

LIQUID CRYSTALS, 1999, VOL. 26, NO. 6, 931–937

Detailed experimental investigation on recording of switchable diffraction gratings in polymer dispersed liquid crystal films by UV laser curing

D. DUCA, A. V. SUKHOV† and C. UMETON*

Istituto Nazionale per la Fisica della Materia (INFM), Unità di Cosenza and
Dipartimento di Fisica, Universita della Calabria,
87036 Arcavacata di Rende (CS), Italy
† Institute for Problems in Mechanics, Russian Academy of Science,
101 pr. Vernadskogo, Moscow 117526, Russia

(*Received 27 July 1998; in final form 30 November 1998; accepted 16 December 1998*)

Results on UV recording of diffraction gratings in polymer dispersed liquid crystal (PDLC) films made with commercially available components are presented. Gratings have been recorded during the curing process by exposing the pre-PDLC mixture to a UV laser interference pattern. The grating morphology, as well as the temporal evolution of the diffraction efficiency, have been experimentally investigated to determine their dependence on curing intensity, liquid crystal concentration and spatial period of the grating. In optimal conditions the resulting diffraction efficiency of the first diffracted beam achieved its theoretical limit for transparent gratings, that is 33%. Possibilities of volume (reflective) grating recording in these materials are also discussed.

1. Introduction

Since the pioneering work of Sutherland *et al.* [1, 2], the utilization of polymer dispersed liquid crystals (PDLCs) for the realization of electrically switched diffraction and holographic gratings has become one of the main items of interest in the area of PDLC-based electro-optical devices. The reason for this interest lies in the possibility of obtaining reliable, cheap and commercial elements for switchable holographic devices [1, 3]; indeed, up to date reported results concern the interesting realization of switchable holographic storage in PDLC [4]. New attempts are continuously being made therefore to obtain good switchable gratings in a variety of different PDLC systems which can utilize simple, commercially available components, and require simple processing. The results reported in this paper represent just one of these attempts.

2. Experimental

We have used the E7 nematic mixture (by Merck) diluted in the well-known [5, 6] NOA65 UV-curable optical adhesive (by Norland): the system is a thiolene-based pre-PDLC mixture, whose properties under spatially-uniform UV curing (by conventional UV lamp radiation) have been studied in detail [5–7]. Furthermore, this mixture has also attracted some attention with regard to the possibility of writing diffraction gratings, and some investigations in this direction have already been carried out with the addition of a small amount of dye to the sample and the use of visible radiation [8, 9]. We have used different liquid crystal mass concentrations C, which range in the interval 20–65 wt %. The lower limit corresponds to the highest value of E7 concentration which is thermodynamically stable in the polymerized sample (i.e no nematic droplets appear in the cured sample, which in such case is not a PDLC sample). The upper limit of the range corresponds to the highest value of E7 concentration which is still stable in the pre-PDLC mixture (i.e. for C values higher than 65 wt %, phase separation occurs spontaneously without curing, and leads to the formation of macroscopic inhomogeneities within the sample). These limits refer to room temperature (20 ± 1°C), at which our experiments have been carried out.

The sample cells were made using two ITO-coated glass slabs, with thickness (20 μm) controlled by appropriate mylar spacers. The mixture preparation and cell filling techniques (at room temperature) were very simple,

* Author for correspondence; e-mail: umeton@fts.unical.it

since no vacuum or nitrogen atmosphere was required. Uncured samples showed good stability: about one week of shelf-life with no observable changes in the properties.

The optical set-up used for UV curing and diffraction efficiency measurements is presented in figure 1. The light beam from an Ar-ion laser (Coherent Innova 90C), operating at the wavelength $\lambda_B = 0.33\,\mu m$ in the power range $3 \rightarrow 100\,mW$, is broadened by the beam expander BE up to a diameter of about 25 mm; it is then divided into two beams of nearly equal intensities ($I_1/I_2 = 0.95 \pm 0.02$) by the beam splitter BS. These beams intersect in the plane of the tuneable aperture I, thus providing an interference pattern whose space period Λ lies in the range $3 \rightarrow 11\,\mu m$. Different Λ values are obtained by changing the intersection angle of the two beams (that is by readjusting the BS mirrors). The polarization is s-type, i.e. the **E** vector is directed along the fringe pattern. The tuneable aperture is used to cut off the wings of the laser beam intensity profile, so that for a spot with a diameter of $2 \rightarrow 5\,mm$, the intensity is uniform within a 5% accuracy. This set-up also enables the curing beam diameter to be changed without noticeably changing the value and the uniformity of the curing intensity. Furthermore, in order to avoid undesirable spatial modulations due to Fresnel diffraction through the aperture I, a 1:1 image of the aperture is created by the lens IL at the entrance plane of the sample; it has also been checked that this lens does not introduce any appreciable degradation in the quality of the impinging beam. The temporal evolution of the diffraction efficiency of the grating is monitored by the probing red light coming from a low power He-Ne laser (about 1 mW at $\lambda_R = 0.63\,\mu m$, the choice of this wavelength being because it is not absorbed by the sample). This probe beam, which is also s-polarised, is slightly focused on the sample (about 1 mm of spot diameter) and the intensities of both transmitted (zero order) and first diffracted (first order) beams are detected by photodiodes ($PD_{t,d}$) and visualized on the oscilloscope. Their efficiencies (η_0 and η_1, respectively) are calculated by using, as reference, the red light intensity which was initially transmitted by the sample, before the curing UV interference pattern is switched onto it.

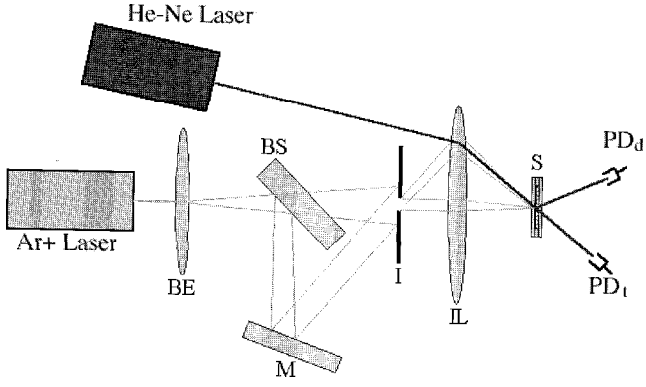

Figure 1. Sketch of experimental set-up. BE = beam expander; BS = beam splitter; I = tuneable aperture; IL = imaging lens; S = sample; $PD_{t,d}$ = photodetectors for transmitted and first order diffracted probe beams, respectively; M = mirror; L = lens.

The morphology of the gratings obtained is checked by an optical polarization microscope with a resolution of about 0.5 μm, whose images are digitally detected by a CCD camera (TCM 112 by GDS).

As for switching measurements, they were carried out in the same geometry (of course, without the UV irradiation) by utilizing the amplified 100 Hz bipolar meander output of a signal generator (33120A by HP). Everywhere below, the term 'switching voltage' refers to the amplitude of this bipolar meander output. No d.c. offset was used except for measurements of the switching relaxation time, which were carried out by using the amplified unipolar meander output of the same generator.

3. Results and discussion

As a general feature we stress that within the above mentioned range of liquid crystal concentrations and grating spacings, gratings with a minimum diffraction efficiency $\eta_1 = 1\%$ have been successfully obtained. Optimal curing conditions (both intensity and duration of the UV irradiation), as well as morphological features and diffraction efficiency, vary considerably however across these ranges (in a quite reproducible manner). Therefore, in order to get a systematic insight into the problem, we describe in detail the morphology, the temporal evolution of the diffraction efficiency and the switching characteristics.

3.1. *Morphological features*

Morphology undergoes evident changes during the UV exposure; the investigation of this temporal evolution of morphology is however beyond the scope of this paper and will be reported elsewhere.

By varying C and Λ, the final morphology of the sample varies both from the point of view of phase separation and anisotropy. Typical (and reproducible) pictures taken at different C values are presented in figure 2. They all refer to the same spacing $\Lambda = 11\,\mu m$ and have been taken using crossed polarizers (whose axes are, respectively, vertical and horizontal in the picture). Figure 2(*a*) represents the $\eta_1 = 1.5\%$ grating in the $C = 20$ wt % sample. It is an isotropic and purely phase grating revealing that no LC droplets exist, at least at a 0.5 μm scale. As already mentioned, this corresponds

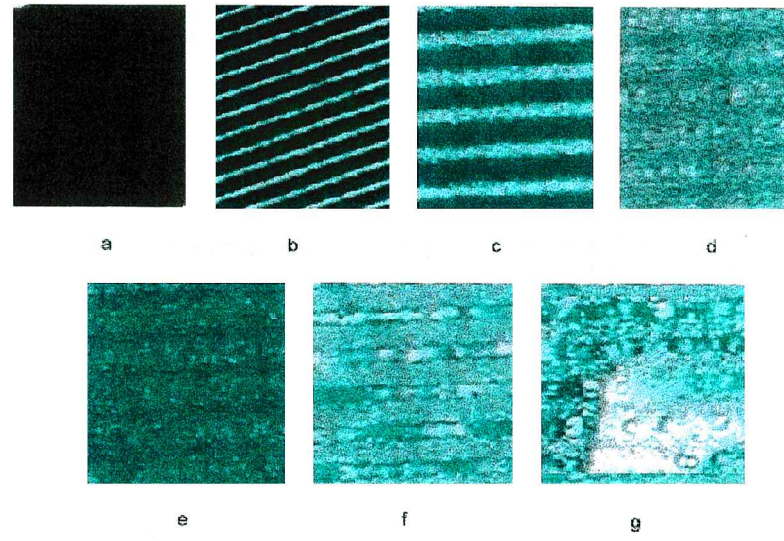

Figure 2. Grating morphology for samples with different liquid crystal concentrations: (*a*) $C = 0.2$; (*b*) $C = 0.25$; (*c*) $C = 0.3$; (*d*) $C = 0.35$; (*e*) $C = 0.4$; (*f*) $C = 0.6$; (*g*) again $C = 0.6$. In all samples the fringe spacing is $\Lambda = 11\,\mu m$. Pictures were taken 20 h after curing, except for (*g*)—see text.

to the fact that the concentration used is thermodynamically stable in the cured polymer. This grating proved not to be switchable by an external voltage; its origin probably lies in a different polymer chain length in the maxima and in the minima of the interference pattern (different stable concentration of excited initiator) and the study of this mechanism is beyond the scope of this paper. In figure 2 (*b*), the $\eta_1 = 16\%$ grating in the $C = 25$ wt % sample is presented. Here and further on, the oblique fringes indicate that the sample is anisotropic, its symmetry axis being parallel or perpendicular to the fringes of the grating. We see an isotropic background containing no micron-scale droplets and 2 μm wide straight-edge stripes, containing a set of nematic droplets of about 1.5 μm diameter, all close to one another. The droplets are birefringent, the axes of about 85% of them being normal to the fringes (checked by a compensator). Figure 2 (*c*) refers to the $\eta_1 = 33\%$ grating in the $C = 30$ wt % sample. This consists of isotropic polymer and classical PDLC stripes. These latter have a width of about 4 μm, filled with nematic droplets of about 1.5 μm diameter and separated by some kind of 'distorted polymer' spacers. The stripe edges are less sharp than in the $C = 25$ wt % case, some of the nematic droplets tending to penetrate into the polymer stripes. PDLC stripes are stochastically birefringent, in the sense that the directors of different nematic droplets are aligned stochastically with respect to each other. In the following, we will refer to this concentration value ($C = 30$ wt %) as the 'optimal' concentration. Figure 2 (*d*) refers to the $\eta_1 = 2.5\%$ grating in the $C = 35$ wt % sample. Now no pure isotropic polymer stripes are present, but only a continuous stochastically birefringent PDLC phase. The observed spatial modulation is concerned only with the

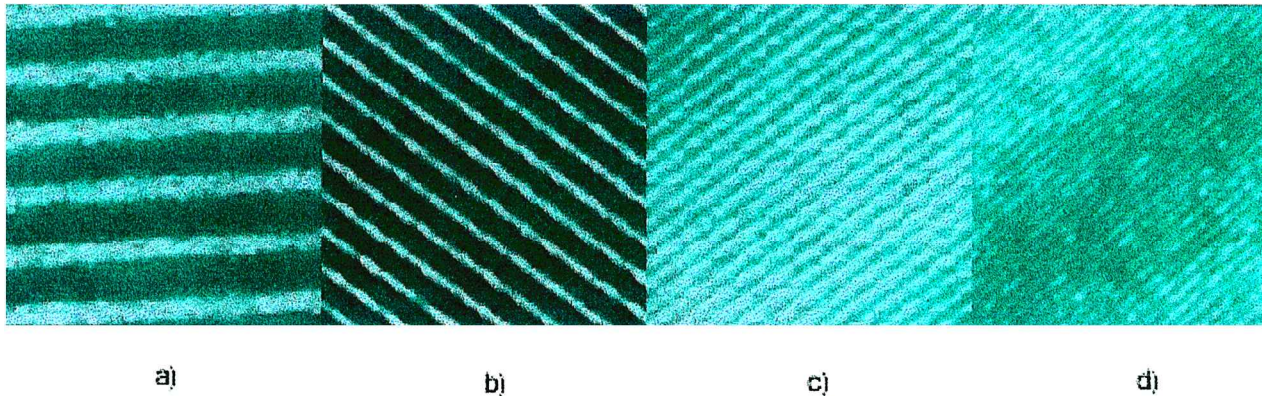

Figure 3. Grating morphology of samples with $C = 0.3$ and different fringe spacing: (*a*) $\Lambda = 11\,\mu m$; (*b*) $\Lambda = 7\,\mu m$; (*c*) $\Lambda = 4.5\,\mu m$; (*d*) $\Lambda = 3.5\,\mu m$.

average size of the nematic droplets. This size is more or less homogeneous and about 1.5 μm, in the 'droplet-poor' stripes, while it reaches values up to 3 → 4 μm in 'droplet-rich' stripes. Figure 2 (*e*) depicts the $\eta_I = 1\%$ grating in the $C = 40$ wt % sample. There is nothing new with respect to the previous case, but the ratio between stripe widths ('droplet rich'/'droplet poor') is now changed: about 1:1 for the $C = 35$ wt % sample and 7:3 for the $C = 40$ wt % sample, in which the 'rich stripe' droplet size is enhanced to 5 → 6 μm. Finally, figure 2 (*f*) refers to the $\eta_I = 0.5\%$ grating in the $C = 60$ wt % sample. Here we see a sequence of PDLC stripes alternated with stripes of huge 'nematic cigars' (3 → 4 μm wide and up to 20 μm long), which are randomly aligned. Figure 2 (*g*) is discussed below.

Where morphology dependence upon the grating spacing Λ is concerned, picures are presented in figure 3, which refers to the optimal liquid crystal concentration $C = 30$ wt %. It can be seen that the difference between the cases of high Λ values [11 → 7 μm, figure 3 (*a*) and (*b*)] and low Λ values [4.5 → 3 μm, figure 3 (*c*) and (*d*)] lies in the orientational properties of the PDLC stripes. As far as the stripe width remains large compared with the droplet size, the stripe remains stochastically aligned. When the stripe width becomes comparable to the droplet size, the droplets in the stripe are oriented perpendicular to it, as was the case for the sample with $C = 25$ wt % and $\Lambda = 11$ μm figure 2 (*b*).

To conclude the morphology description, it should be noted that for liquid crystal concentrations far from the 'optimal' value $C = 30$ wt %, a slow post-curing degradation of the pattern occurs in about one week. In the case of nematic-rich mixtures, huge nematic droplets appear, which overflow several grating fringes; (see figure 2 (*g*) for the $C = 60$ wt % sample). Similarly, big polymer droplets appear in nematic-poor ($C = 25$ wt %) samples.

The above reported results exhibit the following general features of the grating morphology dependence upon the liquid crystal concentration and the fringe spacing:

(1) The mean droplet size remains almost the same (1.5 → 2 μm) until the nematic concentration is low enough to allow pure polymer isotropic stripes to form during the curing process; $C < 35$ wt %, see figure 2 (*b*), 2 (*c*). These mixtures provide the best values of diffraction efficiency.

(2) Droplets are aligned perpendicularly to the polymer fringes as far as the droplets remain contacting the fringes on both sides, i.e. as far as the width of the droplet-containing stripes is about 1 droplet diameter, figure 2 (*b*). The alignment becomes immediately stochastic as soon as this width exceeds the droplet size by a factor of 2 or more, figure 2 (*c*). This is evident in figure 3 where, by varying only Λ for the same C value, we have obtained both stochastic (*a*) and uniform (*b*, *c*, *d*) alignment of the main axes of the droplets.

It is quite reasonable to argue that the above mentioned droplet size (1.5 → 2 μm) is the minimum that is thermodynamically allowed for the given mixture composition. Reduction of this minimum size is necessary to achieve a smaller fringe spacing (as needed, for instance, to obtain reflecting Bragg gratings). In order to make a reasonable pediction about the final grating morphology and efficiency, at least a phenomenological model would be required for the diffusion/condensation kinetics during the curing process. Such a model is at present under development.

3.2. *Temporal evolution of the diffraction efficiency*

We have performed many measurements under different experimental conditions and for different values of the curing intensity I_0 (here and below, I_0 denotes the sum of the intensities of the two interfering beams: $I_0 = I_1 + I_2$). As a general feature, we have found that for each set of experimental conditions, an optimal intensity I_{opt} exists, which enables us to obtain the highest η_I value consistently under these conditions. The value of I_{opt} depends significantly upon C and, to a less extent, upon Λ. These dependences are shown in figure 4 for two extreme values of Λ. It can be seen that I_{opt} is high for concentration values which are close to the 'optimal' concentration, and low elsewhere.

The temporal evolution of diffraction efficiency reveals the same qualitative shape for all the curing intensities which have been used, differing only in the final values achieved. This can be seen in figure 5, where results are

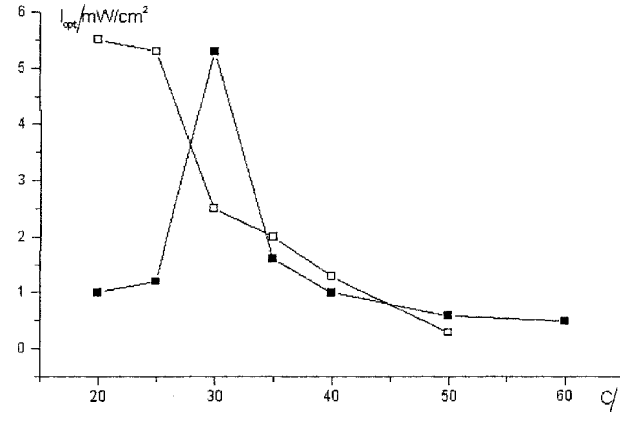

Figure 4. Dependence of the optimal curing UV intensity I_{opt} on the liquid crystal concentration. Black squares refer to a fringe spacing $\Lambda = 11$ μm; open squares refer to $\Lambda = 3.5$ μm.

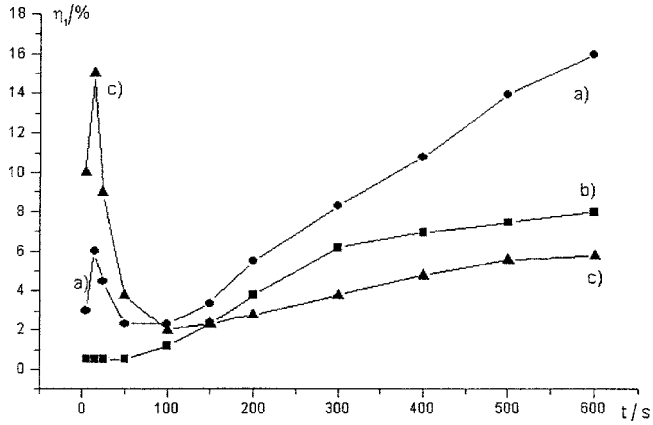

Figure 5. Temporal evolution of the diffraction efficiency η_1 of the $\Lambda = 11\,\mu m$ grating in samples with $C = 0.25$, but cured at different UV intensities: (*a*) $I_0 = 1.06\,mW\,cm^{-2}$; (*b*) $I_0 = 0.53\,mW\,cm^{-2}$; (*c*) $I_0 = 5.3\,mW\,cm^{-2}$.

presented for three different I_0 values, which vary within one order of magnitude ($\Lambda = 11\,\mu m$ and $C = 25$ wt % are fixed for all samples). Furthermore, one more feature has to be pointed out. For mixtures of non-optimal concentration, the temporal evolution of η_1 is not monotonous, as in figure 5 (*b*). An initial peak occurs, in which η_1 achieves a value of 10% or more, even for samples in which the final steady state η_1 value does not exceed 1%. We emphasize that all attempts made to stop the curing process in the maximum of the peak have failed; once the peak is almost reached, further evolution occurs in nearly the same manner, no matter whether the UV irradiation is switched on or off. Our idea is that the dynamics of η_1 are strongly affected by the process of diffusion of excited monomers which, in fact, undergo polymerization while diffusing; theoretical work is in progress with the aim of elaborating a model which could explain the observed η_1 dynamics.

In figure 6, the temporal evolution of η_1 is presented only for the case $I = I_{opt}$ at different C values. All results refer to $\Lambda = 11\,\mu m$. We note that for samples in which C is close to the 'optimal' value, η_1 approaches the theoretical limit for transparent phase gratings (33%), and up to 20 orders of diffraction of the probe beam can be observed.

The dependences of the finally achieved η_1 value on C (at fixed $\Lambda = 11\,\mu m$) and on Λ (at the 'optimal' $C = 30$ wt % value) are presented in figure 7. We see that, at a fixed Λ value, η_1 is high only around the optimal concentration. On the other hand, if C is set at its optimal value, η_1 decreases with decreasing fringe spacing; no qualitative changes in the curve shape occur, only the final η_1 value changes.

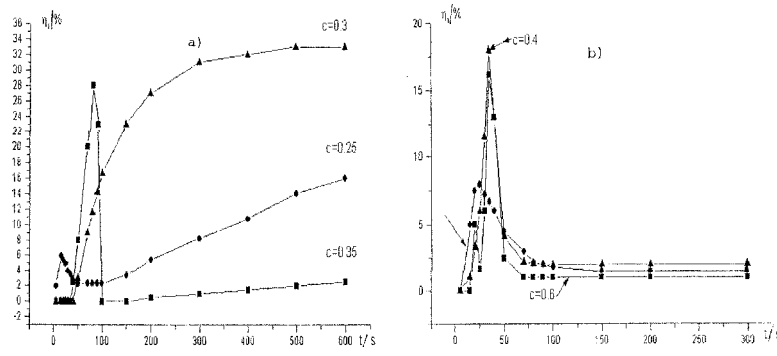

Figure 6. Temporal evolution of the diffraction efficiency η_1 in samples with a liquid crystal concentration which is: (*a*) close to the optimal value; (*b*) far from this value. In all samples the fringe spacing is $\Lambda = 11\,\mu m$.

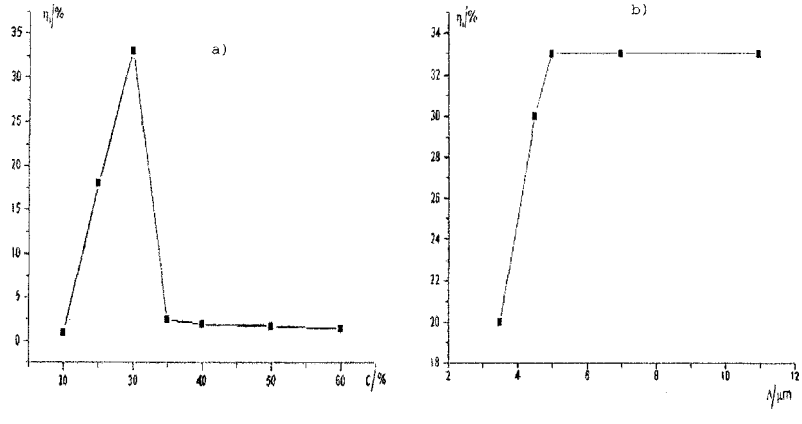

Figure 7. Dependences of the finally achieved diffraction efficiency η_1 upon: (*a*) the liquid crystal concentration, with a fixed fringe spacing $\Lambda = 11\,\mu m$; (*b*) the fringe spacing Λ, with a fixed liquid crystal concentration $C = 0.3$.

Taking into account also the considerations of §3.1 above, we can now state that a good grating is obtained under the following conditions:

(1) The pre-PDLC mixture is a nematic-poor sample, the liquid crystal concentration being too low to allow PDLC formation over all the sample.
(2) The sample is illuminated with a good contrast UV interference pattern of intensity high enough to induce the best condensation of nematic in the maxima of the pattern (thus forming there the smallest possible droplets), but low enough to prevent droplet formation near the minima.

At this stage, an interesting consideration is worth making. The achievement of the theoretical limit $\eta_l = 33\%$ for the diffraction efficiency of the sample with the optimal liquid crystal concentration ($C = 30$ wt %), accompanied by up to 20 visible diffraction maxima, indicates that, between the maxima and minima of the interference pattern, the difference in the optical path of the two interfering beams approximates to $\Delta l = (n + 1/2)\lambda$ (with n an integer), and is not the lowest required value $\Delta l = \lambda/2$. Indeed, in this last case, the intensity of the higher diffraction orders should decrease much faster with increase of the order number. We have estimated the theoretical limit of Δl in a 20 μm thick sample with randomly aligned nematic droplets. This estimation is based on the assumptions that (a) the indices of refraction of the components in the stripes are equal to those of the pure initial components (nematic and polymer); (b) the stripe width corresponds to a half-fringe width. This gives $\Delta l_{\text{lim}} = 5\lambda/2$. Therefore, for samples with $C = 30$ wt %, a thinner cell could probably work as well, which is good from the point of view of any further attempt to reduce the switching time.

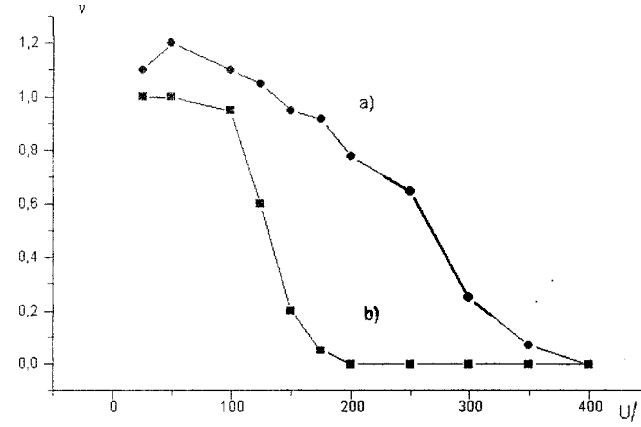

Figure 8. Switching curves for gratings with $\Lambda = 3.5$ μm in samples with liquid crystal concentrations: (*a*) $C = 0.25$; (*b*) $C = 0.3$.

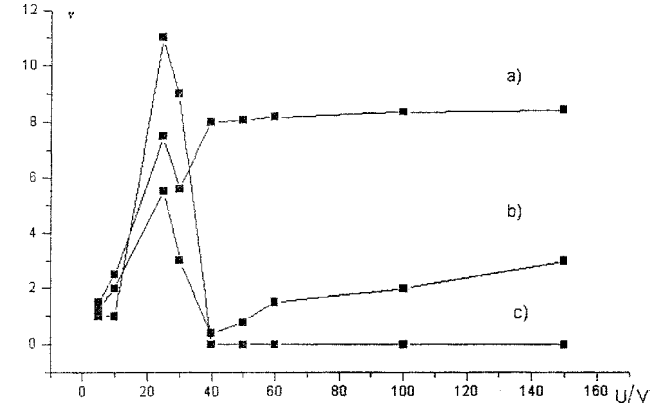

Figure 9. Switching curves in samples with liquid crystal concentration $C = 0.35$ and fringe spacings: (*a*) $\Lambda = 11$ μm; (*b*) $\Lambda = 4.5$ μm; (*c*) $\Lambda = 3.5$ μm.

3.3. *Switching characteristics*

Switching curves could be obtained only for samples in which the liquid crystal concentration was close to the optimal value. The dependence of the normalized diffraction efficiency $\nu = \eta_l(U)/\eta_l(0)$ upon the applied voltage U is presented in figure 8 for samples with $C = 25$ and 30 wt %. The switching voltages obtained are not low (20 V μm^{-1} for $C = 25$ wt % and 10 V μm^{-1} for $C = 30$ wt %), but the relaxation times are quite satisfactory (about one millisecond) and quite independent of the fringe spacing Λ. Indeed these curves refer to the samples with $\Lambda = 3.5$ μm, but they remain almost the same for all measured values of Λ. Curves referring to the $C = 35$ wt % samples are presented in figure 9 for different Λ values, and show interesting differences from the curves of figure 8: (a) in some case, the diffraction efficiency is not switched off by increasing U, but rather enhanced by a factor of 10; (b) the required voltages are about one order of magnitude lower than for previous C values—in this case we have also noted that, when a unipolar meander is applied, ν changes by a factor of 3 and more if the meander sign is changed.

Finally, a plot of the dependence of relaxation time on liquid crystal concentration is presented in figure 10. We see that, in the $C = 35$ wt % sample, the relaxation time is about two orders of magnitude higher than in the other cases: $\tau_{35\%} \approx 0.5$ s; this value exceeds by a factor of 5 the relaxation time of a pure nematic cell of the same thickness. The unusual behaviour shown in figure 9, as well as the dependence of ν on the sign of the applied voltage and the high value of $\tau_{35\%}$, in our opinion indicate that: (a) an initial pretilt of the liquid crystal director with respect to the cell slabs must be present in the $C = 35$ wt % samples; (b) the existence of an intrinsic electrostatic field in the sample could be the reason for such a pretilt.

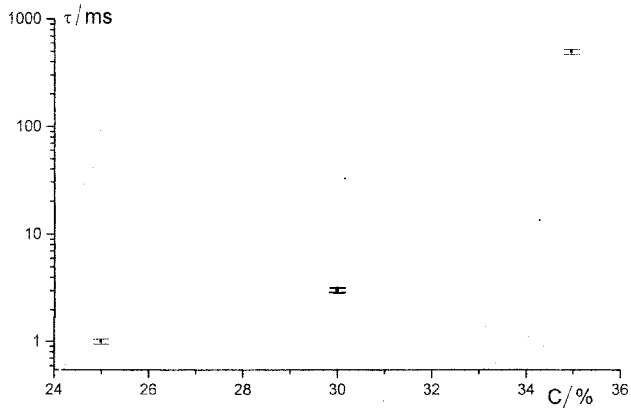

Figure 10. Dependence of the switching relaxation time τ on the liquid crystal concentration C (a logarithmic scale has been used in the y-axis).

These considerations have induced us to check the response of the same samples to a d.c. field. Only a transient change in the diffraction efficiency was found, but its final value was not affected by the applied d.c. voltage; therefore we argue that nematic droplets are somehow conductive. The estimated conductivity required to provide a Maxwell's relaxation time equal to $\tau_{35\%}$ is about $10^{-7}\ \Omega^{-1}\,\mathrm{cm}^{-1}$. This value of conductivity is just sufficient to produce in the droplets a complete screening of an external field and prevent their reorientation. This kind of 'photorefractive feature' observed in these samples encourages a separate and detailed investigation of the argument.

The switching voltages of good gratings (figure 8) are not the best values known today [1–4]. The relaxation times obtained $\tau \approx 1$ ms (figure 10) are however quite satisfactory and encouraging for the possibility of improving the switching parameters. In particular, we think that the utilization of some surfactant could decrease both the isotropic and the anisotropic parts of the tension per unit surface σ. A decrease of the isotropic part leading, let us say, to a decrease by N times of the droplet size, and hence to an increase by N times of the switching voltage, should lead also to a decrease of N^2 times in τ. If sumultaneously it would be possible to obtain a high enough decrease of the anisotropic part of σ to produce an increase of N^2 times in τ, we should again get the initial satisfactory value of the switching time but, on the other hand, the switching voltage would decrease by N^2 times, thus becoming N times lower than the initial value.

4. Conclusions

We have performed a detailed experimental investigation of switchable diffraction gratings recorded in polymer dispersed liquid crystal films by UV laser curing. Our attempts have been devoted to the possibility of obtaining good switchable gratings in PDLC systems which can utilize simple, commercially available components, and require a simple processing. Pre-PDLC mixture compositions investigated in this paper appear to be quite satisfactory media for this purpose and, in particular, for the formation of transparent switchable diffraction gratings, in which the highest theoretical value of the diffraction efficiency has been achieved. The possibilities of obtaining a further increase of the spatial resolution (which could allow the formation of Bragg holographic gratings) and a decrease in switching voltages have been also discussed. We hope that in the near future we will achieve such improvements. In addition, the results obtained reveal two new items of interest, which encourage further investigation: the initial peaks observed in the temporal evolution of the diffraction efficiency of some samples and a photorefractive switching behaviour observed in some nematic-rich samples.

The authors are grateful to Drs N. V. Tabiryan, G. Cipparrone, A. Mazzulla and V. Lazarev for helpful discussions, comments and some experimental support. The work has been carried out with the support of the European Community through the European Fund of Regional Development, in the frame of 'Progetto Sud INFM', sub-project FESR-UME.

References

[1] Sutherland, R. L., Tondiglia, V. P., Natarajan, L. V., and Bunning, T. J., 1993, *Chem. Mater.*, **5,** 1533.
[2] Sutherland, R. L., Tondiglia, V. P., and Natarajan, L. V., 1994, *Appl. Phys. Lett.*, **64,** 1074.
[3] Sutherland, R. L., Tondiglia, V. P., Natarajan, L. V., Bunning, T. J., and Adams, W. W., 1996, *J. nonlinear-Opt. Phys. Mater.*, **5,** 89.
[4] Sutherland, R. L., Tondiglia, V. P., Natarajan, L. V., Bunning, T. J., and Adams, W. W., 1995, *Opt. Lett.*, **20,** 1325.
[5] Smith, G. W., 1991, *Mol. Cryst. liq. Cryst.*, **196,** 89.
[6] Lovinger, A. J., Amundson, K. R., and Davis, D. D., 1994, *Chem. Mater.*, **6,** 1726.
[7] Di Bella, S., Lucchetti, L., and Simoni, F., *Mol. Cryst. liq. Cryst.* (to be published).
[8] Fuh, A. Y.-G., Huang, C.-Y., Tsai, M.-S., Chen, J.-M., and Chien, L.-C., 1996, *Jpn. J. appl. Phys.*, **35,** 630.
[9] Fuh, A. Y.-G., Tsai, M.-S., Liu, T.-C., and Chien, L.-C., 1997, *Jpn. J. appl. Phys.*, **36,** 6839.